All-optical signal amplification in multiple-quantum-well resonant photonic bandgap structures

S. Schumacher,[a] N. H. Kwong, and R. Binder
College of Optical Sciences, University of Arizona, Tucson, Arizona 85721, USA

(Received 10 January 2008; accepted 11 March 2008; published online 1 April 2008)

Using a microscopic many-particle theory, we predict all-optical amplification of low-intensity light pulses in resonant photonic bandgap structures realized by Bragg-spaced semiconductor multiple quantum wells. The discussed scheme is based on mirrorless parametric amplification. © *2008 American Institute of Physics*. [DOI: 10.1063/1.2904696]

Monolithic-integrated photonic bandgap structures[1] (PBGs) play an increasingly important role in optical communication systems. Implemented in many different physical realizations, they allow for use in advanced application schemes (for example, optical buffers[2]). An important aspect that still may benefit from further conceptual investigations is that of all-optical light amplification. Here, we present a theoretical proposal for amplification in a resonant PBG (RPBG), in which the photonic bandgap is spectrally close to an optical resonance present in each unit cell. Our specific implementation of the RPBG is that of a multiple-quantum-well RPBG (MQW-RPBG) with excitonic resonances.[3–7] We predict optical gain and temporal instabilities (analogous to the "mirrorless optical parametric oscillator[8,9]"). Our scheme is a promising alternative to existing amplification schemes (based on stimulated Raman scattering[10–12]). Depending on device design requirements, potential drawbacks of our proposal, e.g., the need for narrow exciton resonances, may be outweighed by its predominant advantage of large achievable gain in a very small (micron-sized) system.

All-optical amplification of weak light pulses can be achieved in systems with or without mirrors. Amplification and optical instability without mirrors were proposed three decades ago[8] and were recently demonstrated in solid state systems.[9] On the other hand, strong amplification in a system with mirrors has been demonstrated for exciton polaritons in semiconductor microcavities.[13–18] It is natural to ask whether amplification, similar to the case of cavity polaritons, can also be achieved without mirrors. In the microcavity, the coupling of the excitonic resonances of the QW to the confined optical modes in the cavity leads to the formation of an in-plane (parallel to the QW plane) dispersion with lower and upper polariton branches (LPB and UPB, respectively). In the strong coupling regime, this dispersion strongly differs from the bare in-plane cavity and exciton dispersions. The LPB is spectrally pulled well below the bare QW exciton resonance and control pulse produced excitation-induced dephasing (EID) from two-exciton correlations is strongly suppressed in this spectral region.[19,20] This is crucial for the polariton amplification to occur.[21]

Whereas in planar microcavities the propagation parallel to the plane of the embedded QW is important for the polariton amplification, in MQW structures the radiative coupling of the QWs also leads to polariton effects for propagation perpendicular to the QW planes.[22,23] For inter-QW distances close to Bragg spacing, i.e., half the optical wavelength of the QW excitons, a one-dimensional RPBG is formed (cf. Fig. 1). For excitation close to the lower stop-band edge of the MQW-RPBG, EID from polariton-polariton scattering is strongly suppressed due to the reduced density of available scattering states in this energy region[24] (cf. Refs. 19 and 20). We take advantage of this suppression of EID and show how in a MQW-RPBG strong four-wave mixing (FWM) induced amplification of polaritons can be achieved in a typical setup with control and signal pulses [cf. Fig. 1(a)].

In the framework of our theoretical approach, we solve the coupled equations of motion for the optically induced signal, idler, and control polarizations in each QW. The dynamics of these polarizations is calculated self-consistently together with the time-dependent propagation of the optical fields inside the structure. Via this self-consistent solution of exciton-polarization dynamics and Maxwell's equations, the exciton-exciton interactions which are local in each QW lead to the effective polariton-polariton interaction. The many-particle part of our theory is based on the dynamics-controlled truncation approach[25,26] and includes all coherent optically induced third order nonlinearities, i.e., phase-space-filling (PSF), excitonic mean-field [Hartree–Fock (HF)] Coulomb interaction and two-exciton correlations on a microscopic level. We use a two-band model (including spin-degenerate conduction and heavy-hole valence band) with the circular dipole selection rules for quasinormal incidence

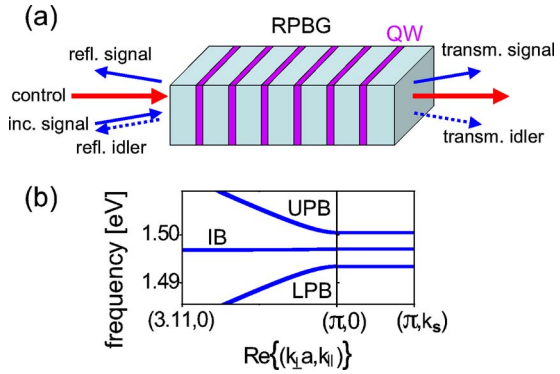

FIG. 1. (Color online) (a) Excitation geometry of a MQW-RPBG. (b) Photonic band structure for an infinite Bragg-spaced MQW (the inter-QW distance is a), showing the intermediate band (IB), the stop-band regions, and the two polariton bands spectrally above (UPB) and below (LPB) the stop-bands. The dependence of the bandstructure on the in-plane momentum $k_{\|}$ is neglected for the considered small angles of incidence related to the in-plane momentum k_s.

[a]Electronic mail: sschumacher@optics.arizona.edu.

for the optically induced interband transitions in the GaAs QWs.[27,28] Restricting to excitation spectrally below the bare exciton resonance, we account for the dominant contributions to the coherent optical response by evaluating the polarization equations in the $1s$ heavy-hole exciton basis.[29,30] The propagation of the light fields is included via a time-dependent transfer matrix approach[31] that in the linear regime for an infinite MQW-RPBG gives the polariton bandstructure shown in Fig. 1(b). We apply an in-plane momentum decomposition of field and polarization: the control has zero in-plane momentum $k=0$ and we chose the finite (although small) in-plane momenta k_s and $-k_s$ for signal and idler, respectively. The in-plane dispersion of the excitons is neglected along with possible small changes to the polariton dispersion for signal and idler not strictly propagating in normal incidence.[24] For the future, it would be worthwhile to study the polariton amplification in MQW-RPBGs for oblique pump excitation ($\gtrsim 10°$ external angle), explicitly considering the polariton in-plane dispersion. We go beyond an evaluation of the theory on a strict $\chi^{(3)}$ level by self-consistently calculating the exciton and two-exciton-polarization dynamics up to arbitrary order in the optical field (the equations are linearized in the weak signal field).[21,30] Correlations involving more than two excitons and those involving incoherent excitons are neglected. These effects are not expected to qualitatively alter the presented results for the considered coherent exciton densities of $\sim 10^{10}$ cm^{-2} for excitation well below the exciton resonance. We concentrate on cocircular ($\sigma_+\sigma_+$) excitation and keep the discussion of spin-dependent polariton scattering for the future.[32] Semiconductor to air transitions at the ends of the structure which we included in this study generally lower the threshold. However, this "mirror effect" or "cavity enhancement" is not required for the reported amplification. In a schematic representation, the nonlinear equations of motion for the excitonic polarizations in each QW in signal (k_s) and idler ($-k_s$) directions read $i\hbar\dot{p}_{\pm k_s}=\tilde{\varepsilon}p_{\pm k_s}+\tilde{\Omega}_{\pm k_s}+V_{\mathrm{HF}}p_0p_0p^*_{\mp k_s}+\mathrm{PSF}+\mathrm{corr}$. Here, p_0 is the pump-induced exciton polarization, $\tilde{\varepsilon}$ the $1s$ exciton energy including the dephasing constant γ and nonlinear energy shifts, $\tilde{\Omega}_{\pm k_s}$ is the bleaching-corrected Rabi energy, V_{HF} is the HF Coulomb matrix element in the $1s$ exciton basis, and "PSF" and "corr." denote nonlinearities arrising from PSF and two-exciton correlations, respectively [for more details, see, e.g., Eq. (1) in Ref. 21].

In cocircular excitation configuration, we obtain the results shown in Fig. 2 for two different MQW-RPBGs with 200 and 400 QWs, respectively. The linear optical properties are depicted in panels (a) and (a′). Panels (b)–(e) and (b′)–(e′) show the signal and idler gain, $(F^{\mathrm{signal,idler}}_{\mathrm{refl.}}+F^{\mathrm{signal,idler}}_{\mathrm{transm.}})/F^{\mathrm{signal}}_{\mathrm{inc.}}-1$, for different control frequencies around the lower stop-band edge. Parameters are noted in each panel and in the figure caption. $F^{\mathrm{signal,idler}}_{\mathrm{refl.,transm.,inc.}}$ is the time-integrated reflected, transmitted, or incoming signal or idler intensity, respectively. For control excitation close to the effective polariton resonance near the lower stop-band edge, for the 400-QW structure, almost two orders of magnitude of spectrally integrated signal and idler gain are found in Fig. 2(b). This gain is strongly peaked at a specific control frequency where excitation with the spectrally narrow control pulse allows for resonant stimulated scattering of control polaritons on the (HF blueshifted) polariton dispersion of

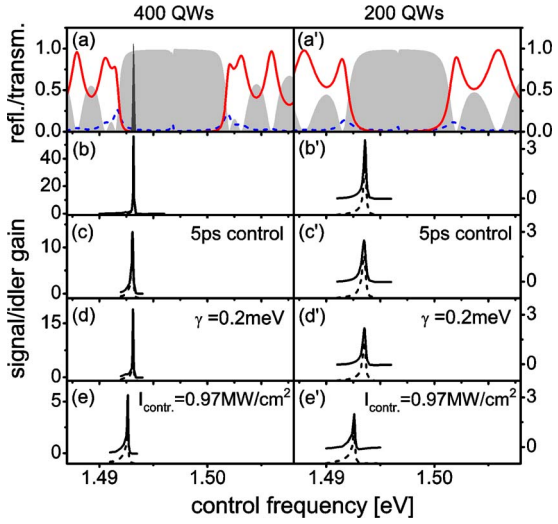

FIG. 2. (Color online) Gain in the Bragg-spaced MQW structures. Left: 400-QWs, right: 200-QWs. [(a) and (a′)] Linear reflection (gray shaded), transmission (solid), and absorption (dashed). (a) Included is the spectral shape of the control pulse (dark gray shaded) for the optimum control frequency in (b). [(b)–(e) and (b′)–(e′)] Gain in the signal (solid) and idler (dashed) directions vs the central control frequency (same as central signal frequency). Note the different scales of the vertical (gain) axes in the left column. Results are shown for Gaussian control and signal pulses of 10 and 1 ps length full width at half maximum, respectively. The control to signal delay time is zero. The control peak intensity is $I_{\mathrm{control}}\approx 2.49$ MW cm^{-2} and the exciton dephasing is $\gamma=0.1$ meV. Deviations from these parameters are noted in each panel.

signal and idler. Note that in Fig. 2(b), this peak in the gain is spectrally narrower than the control spectrum itself. Calculations not represented in Fig. 2 show that the phase-conjugate FWM induced gain is sufficient to overcome intrinsic and radiative losses of the QW polarizations so that the unstable regime is reached. Once the system is unstable, the signal and idler gain grow almost exponentially with the control pulse length as long as the scattering into the signal and idler beams does not significantly influence the control pulse. In the unstable regime the gain is strongly reduced by reducing the control pulse duration from 10 ps [panel (b)] to 5ps [panel (c)]. It is also reduced by choosing less favorable parameters [panels (d) and (e)]. As shown in panels (b′)–(e′), for the shorter 200-QW structure, only moderate amounts of gain are found. The effective polariton resonances in this structure are not sufficiently pronounced to reach the unstable regime for any of the cases shown.

Although large optical gain that increases with the control pulse duration [cf. panels (c) and (b) of Fig. 2] is indicative of the proposed instability, it does not necessarily imply exponential growth (i.e., instability) in the time domain. We supplement the gain analysis in Fig. 2 by the time domain results shown in Fig. 3(a). These results correspond to the data in Fig. 2(b) around the control frequency where the maximum gain is found. Only signal reflection is shown. Signal transmission and idler transmission and reflection show the same qualitative behavior. Results are shown for three different control frequencies to demonstrate the sensitivity to this parameter. Close to the optimum control frequency, the time-resolved signal reflection shows (almost) exponential growth over a certain time period as long as the control pulse is strong enough to keep the system in the unstable regime [visible for the thick solid line in Fig. 3(a) between 2 and 8 ps]. Away from the optimum control fre-

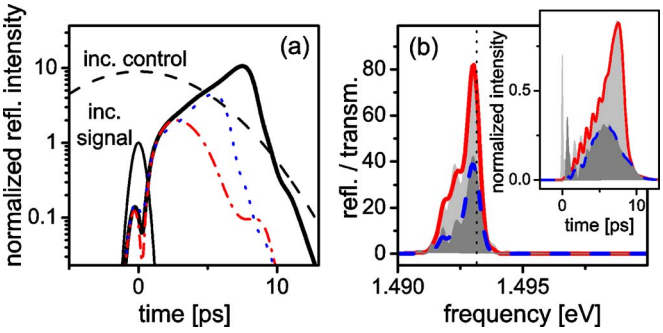

FIG. 3. (Color online) (a) Time-resolved reflected signal intensity (in units of incoming signal's peak intensity), corresponding to the data in Fig. 2(b). Control (thin dashed) and signal (thin solid) central frequencies are 1.493 12 eV (dashed-dotted), 1.493 16 eV (solid), and 1.493 20 eV (dotted). (b) Spectral domain results for signal (light gray shaded) and idler (solid) reflection and signal (dark gray shaded) and idler (dashed) transmission for the optimum control frequency (indicated by dotted line). Calculations done for a spectrally broad 200 fs signal. Inset: corresponding time-resolved reflected and transmitted signal and idler intensities normalized to the incoming signal's peak intensity.

quency, the exponential growth generally has a smaller growth rate and the growth period is shorter (dotted) or the exponential growth is absent where the unstable regime is not reached (dashed dotted). Figure 3(b) shows spectral domain results for the optimum control frequency. Reflectivity and transmission for signal and idler much larger than unity (up to about 80) are seen. Their maxima are found close to the control frequency. We conclude that the dominant contribution stems from (almost) degenerate FWM processes exclusively involving polaritons on the LPB. Our results are also supported by a linear stability analysis (along the lines given in Refs. 8 and 33) for monochromatic steady-state control excitation. The above-investigated instability is enabled by control pulse excitation of the coherent polariton states at the lower stop-band edge in the MQW-RPBG (spectrally well below the bare exciton resonance). Following from the in-plane polariton dispersion[24] in this energy region, the density of final states for scattering of coherent polaritons into states with finite in-plane momentum is small. Thus, two-exciton correlations that weaken the polariton scattering driving the instability and EID losses due to scattering off coherent excitons are strongly suppressed (previously pointed out for microcavity polaritons[19,20]). In a one-dimensional nonresonant PBG, nondegenerate FWM involving photons on different branches of the dispersion was used[34] to achieve efficient frequency conversion. For the MQW-RPBG, an instability relying on interbranch scattering of polaritons may well be inhibited by excessive EID in the UPB.

In summary, based on a microscopic many-particle theory, we predict all-optical amplification of low-intensity light pulses in RPBGs realized by Bragg-spaced semiconductor QWs. The discussed amplification scheme is an example of "mirrorless parametric amplification[8,9]" and may become of interest as an alternative to existing schemes.[10–12] Further interest may be stimulated by an extension to RPBGs of higher dimensionality.

We thank Arthur L. Smirl for generously sharing his ideas and insights on the subject matter with us. This work is supported by ONR, DARPA, JSOP, and by the DFG (SCHU 1980/3-1).

[1] J. D. Joannopoulos, R. D. Meade, and J. N. Winn, *Photonic Crystals: Molding the Flow of Light* (Princeton University Press, Princeton, 1995).
[2] F. Xia, L. Sekaric, and Y. Vlasov, Nat. Photonics **1**, 65 (2007).
[3] E. L. Ivchenko, A. I. Nesvizhskii, and S. Jorda, Phys. Solid State **36**, 1156 (1994).
[4] M. Hübner, J. Kuhl, T. Stroucken, A. Knorr, S. W. Koch, R. Hey, and K. Ploog, Phys. Rev. Lett. **76**, 4199 (1996).
[5] J. Prineas, J. Zhou, J. Kuhl, H. Gibbs, G. Khitrova, S. Koch, and A. Knorr, Appl. Phys. Lett. **81**, 4332 (2002).
[6] M. Schaarschmidt, J. Förstner, A. Knorr, J. P. Prineas, N. C. Nielsen, J. Kuhl, G. Khitrova, H. M. Gibbs, H. Giessen, and S. W. Koch, Phys. Rev. B **70**, 233302 (2004).
[7] Z. S. Yang, N. H. Kwong, R. Binder, and A. L. Smirl, Opt. Lett. **30**, 2790 (2005).
[8] A. Yariv and D. M. Pepper, Opt. Lett. **1**, 16 (1977).
[9] C. Canalias and V. Pasiskevicius, Nat. Photonics **1**, 459 (2007).
[10] J. F. McMillan, X. Yang, N. C. Panoiu, R. M. Osgood, and C. W. Wong, Opt. Lett. **31**, 1235 (2006).
[11] H. Oda, K. Inoue, N. Ikeda, Y. Sugimoto, and K. Asakawa, Opt. Express **14**, 6659 (2006).
[12] H. Rong, A. Liu, R. Jones, O. Cohen, D. Hak, R. Nicolaescu, A. Fang, and M. Paniccia, Nature (London) **433**, 292 (2005).
[13] P. G. Savvidis, J. J. Baumberg, R. M. Stevenson, M. S. Skolnick, D. M. Whittaker, and J. S. Roberts, Phys. Rev. Lett. **84**, 1547 (2000).
[14] R. Huang, F. Tassone, and Y. Yamamoto, Phys. Rev. B **61**, R7854 (2000).
[15] C. Ciuti, P. Schwendimann, B. Deveaud, and A. Quattropani, Phys. Rev. B **62**, R4825 (2000).
[16] M. Saba, C. Ciuti, J. Bloch, V. Thierry-Mieg, R. Andre, L. S. Dang, S. Kundermann, A. Mura, G. Bongiovanni, J. L. Staehli, and B. Deveaud, Nature (London) **414**, 731 (2001).
[17] J. Keeling, F. M. Marchetti, M. H. Szymanska, and P. B. Littlewood, Semicond. Sci. Technol. **22**, R1 (2007).
[18] C. Diederichs, J. Tignon, G. Dasbach, C. Ciuti, A. Lemaitre, J. Bloch, P. Roussignol, and D. Delalande, Nature (London) **440**, 904 (2006).
[19] N. H. Kwong, R. Takayama, I. Rumyantsev, M. Kuwata-Gonokami, and R. Binder, Phys. Rev. Lett. **87**, 027402 (2001).
[20] S. Savasta, O. Di Stefano, and R. Girlanda, Phys. Rev. Lett. **90**, 096403 (2003).
[21] S. Schumacher, N. H. Kwong, and R. Binder, Europhys. Lett. **81**, 27003 (2008).
[22] T. Ikawa and K. Cho, Phys. Rev. B **66**, 085338 (2002).
[23] T. Stroucken, A. Knorr, P. Thomas, and S. W. Koch, Phys. Rev. B **53**, 2026 (1996).
[24] M. V. Erementchouk, L. I. Deych, and A. A. Lisyansky, Phys. Rev. B **73**, 115321 (2006).
[25] V. M. Axt and A. Stahl, Z. Phys. B: Condens. Matter **93**, 195 (1994).
[26] Th. Östreich, K. Schönhammer, and L. J. Sham, Phys. Rev. Lett. **74**, 4698 (1995).
[27] S. Schumacher, G. Czycholl, and F. Jahnke, Phys. Rev. B **73**, 035318 (2006).
[28] The background refractive index is $n_{bg}=3.61$, the effective electron mass $m_e=0.067m_0$, and the effective hole mass $m_h=0.1m_0$. The corresponding exciton binding energy is $E_b^x \approx 13$ meV and the bulk Bohr radius is $a_0^x \approx 170$ Å. The $1s$ exciton energy is $\varepsilon_x=1.4965$ eV, the dipole coupling is $d_{cv}=4\ e$ Å, the dephasing is $\gamma=0.1$ meV, and the Bragg energy is $\varepsilon_{\mathrm{Bragg}}=\varepsilon_x+0.5$ meV$=1.497$ eV.
[29] R. Takayama, N. H. Kwong, I. Rumyantsev, M. Kuwata-Gonokami, and R. Binder, Eur. Phys. J. B **25**, 445 (2002).
[30] M. Buck, L. Wischmeier, S. Schumacher, G. Czycholl, F. Jahnke, T. Voss, I. Rückmann, and J. Gutowski, Eur. Phys. J. B **42**, 175 (2004).
[31] Z. S. Yang, N. H. Kwong, R. Binder, and A. L. Smirl, J. Opt. Soc. Am. B **22**, 2144 (2005).
[32] S. Schumacher, N. H. Kwong, and R. Binder, Phys. Rev. B **76**, 245324 (2007).
[33] W. J. Firth, A. Fitzgerald, and C. Paré, J. Opt. Soc. Am. B **7**, 1087 (1990).
[34] C. Becker, M. Wegener, S. Wong, and G. von Freyman, Appl. Phys. Lett. **89**, 131122 (2006).